GMR
The Original

GC-MS AND FTIR PROFILING OF *SOLANUM NIGRUM* MOTHER TINCTURE: QUALITY CHARACTERIZATION AND MECHANISTIC PLAUSIBILITY MAPPING TO CHRONIC RHINOSINUSITIS PATHOBIOLOGY

Sivadharshini S[1], Shilpa Prasad[2], Vettrivel Arul[3*]

[1*]PG Scholar, Department of Homoeopathic Repertory and Case Taking, Vinayaka Mission's Homoeopathic Medical College & Hospital, VMFRDU, Salem, Tamil Nadu, India, E-mail ID: sivamathi5833@gmail.com
[2]Associate Professor, Department of Homoeopathic Repertory and Case Taking, Vinayaka Mission's Homoeopathic Medical College & Hospital, VMFRDU, Salem, Tamil Nadu, India
[3]Assistant Professor, Department of Community Medicine, Vinayaka Mission's Homoeopathic Medical College & Hospital, VMFRDU, Salem, Tamil Nadu, India

ABSTRACT:
Chronic rhinosinusitis (CRS) is a heterogeneous, long-standing inflammatory disease in which epithelial barrier dysfunction, immune dysregulation, oxidative stress, and microbial persistence interact to sustain mucosal pathology. To enable disciplined mechanistic discussion of complex botanical preparations in CRS, transparent chemical standardization is essential. This study profiled Solanum nigrum homoeopathic mother tincture (Q) using gas chromatography-mass spectrometry (GC-MS) and Fourier transform infrared spectroscopy (FTIR), followed by evidence-mapped mechanistic plausibility appraisal anchored to CRS guideline domains. GC-MS was performed on an Agilent GC 8890/MS 5977C (DB-5MS column) with NIST20 library matching, and FTIR spectra were acquired on a Thermo Nicolet iS5 (KBr pellet; 550-4000 cm^{-1}). The GC-MS profile was dominated by Olean-12-en-3-ol, acetate (3β) (RT 24.1868; Area%-T 23.98) and sugar-related constituents including ethyl α-D-glucopyranoside (RT 14.9447/15.0321; Area%-T 16.51/12.45) and α-L-rhamnopyranose (RT 14.8573; Area%-T 4.11), with a triterpenoid hydrocarbon annotation (24-noroleana-3,12-diene; Area%-T 10.75). FTIR bands at 3332 and 1084-1045 cm^{-1} supported hydroxyl-rich, C-O-dominated chemistry, while 2978 cm^{-1} indicated aliphatic chains. Likely siloxane/plasticizer artifacts were flagged and excluded from CRS mapping. The integrated fingerprint provides a quality baseline for batch comparison and motivates targeted antibiofilm and anti-inflammatory validation in CRS models in clinically relevant settings.

KEYWORDS: Solanum nigrum mother tincture; GC-MS/FTIR chemical profiling; chronic rhinosinusitis (CRS)

INTRODUCTION

CRS is a chronic inflammatory disease of the nasal and paranasal sinus mucosa, presenting with symptoms lasting longer than 12 weeks, and demonstrated through objective signs of mucosal disease. Clinically, CRS is heterogeneous and can be broadly categorized in 2 types: with nasal polyps and without nasal polyps24. However, these phenotypes also share the same pathobiological features. Modern paradigms describe a complex disease process that is characterized by epithelial barrier disruption, abnormal innate and adaptive immunity, oxidative stress and microbe persistence. Biofilm-forming bacteria and chronic mucosal inflammation can interact to mutually aggravate one another, leading to disease chronicity and variability in treatment response22.

The mechanistic basis of CRS offers a strong biological rationale to explore multilineage adjunct therapies. Inflammatory mediated signalling pathways, cytokine aberration and tissue remodelling are crucial in the pathogenesis of oedema, mucous hypersecretion and mucosal injury9. Finally, inflammatory intensity and epithelial integrity can be amplified by oxidative stress. Meanwhile, mucosal imbalances between microbes and biofilm cause chronic stimulations of mucosal immune response against microbial structure, as a result enzyme-mediated strategy of anti-microbe resistance generally may be reduced23. These interlinked characteristics explain limitations in treating CRS with single-mechanism therapies and reflect growing appreciation for chemically complex formulations based on hypothesis-generating mechanistic frameworks.

Herbal extracts and mother tinctures are multi-component systems, which could contain volatile or semi-volatile metabolites, glycosides, fatty acids and terpenoid or triterpenoid derivatives. Numerous of such compounds are reported in the literature for their anti-inflammatory, antioxidant, antimicrobial and anti-biofilm effects11. However, success in generating biological interpretations out of any plant-based medicinal

preparation is largely depending on its strict chemical standardization and clear ex-situ quality profiling. In the absence of a chemical fingerprint, it is difficult to compare batches, evaluate mechanistic plausibility or discriminate between true components and analytical artifacts.

Solanum nigrum has been studied extensively in pharmacognostic and ethnopharmacological literature but differences in its chemical composition are attributed to variables such as plant part, geographical source, extraction solvent and processing method4. Solanum nigrum mother tincture (Q) prepared in homeopathic pharmacy is an ethanolic extract and hence appropriate for its analytical characterization by complementary methods. Gas chromatography-mass spectrometry (GC-MS) enables the screening of volatile and semi-volatile analytes, following tentative identification by spectral library matching. Also, Fourier transform infrared (FTIR) spectral data describes the characteristic functional group profile which accompanies the major bond vibrations of the mixture. In combination, GC-MS and FTIR can generate an intelligible chemical profile enabling quality characterisation which carefully should be related to disease relevant mechanistic areas.

Here, we carried out GC-MS and FTIR analyses on the chemical composition of Solanum nigrum mother tincture, then exercised an interpretation of the identified constituents and functional group pattern in line with the CRS pathobiology. This mechanistic explanation is offered as a map of plausibility but not evidence for clinical efficacy. Recognizing that GC-MS methodologies can sense impurities such as background siloxanes and plasticizer-associated esters, we followed an artifact screening protocol limiting our biological interpretation to components judged likely genuine. The detailed analytical and evidence map integration used in this is aimed at developing a reproducible chemical fingerprint for Solanum nigrum mother tincture and prepares a disciplined base also for discussing its possible mechanistic value in CRS research.

MATERIALS AND METHODS

Study design and analytical workflow

This study was designed as an analytical profiling and quality characterization of Solanum nigrum homoeopathic mother tincture (Q) using Gas Chromatography-Mass Spectrometry (GC-MS) for volatile and semi-volatile constituents and Fourier Transform Infrared (FTIR) spectroscopy for functional group fingerprinting. The workflow comprised GC-MS acquisition and library-based identification, FTIR spectral acquisition using the KBr pellet method, peak extraction, and an evidence-mapped mechanistic interpretation relevant to chronic rhinosinusitis (CRS). A mandatory contamination and artifact-screening step was incorporated to prevent analytical artifacts from being misinterpreted as genuine phytoconstituents.

Sample

Solanum nigrum homoeopathic mother tincture (Q) was analysed as received. The sample identity in the analytical report was “T-25032085-17-R-SOL-PURITY.” The present work reports chemical fingerprints derived from the supplied analytical outputs and interprets findings conservatively as mechanistic plausibility rather than clinical efficacy.

Gas Chromatography-Mass Spectrometry (GC-MS)

Instrumentation and chromatographic conditions

GC-MS analysis was performed using an Agilent GC-MS system (GC 8890 coupled with MS 5977C, Autosampler 7693A, USA). Separation was carried out on a DB-5MS capillary column (30 m × 0.25 mm internal diameter × 0.25 µm film thickness). The oven temperature program began at 50 °C (held for 1 min), increased at 10 °C/min to 300 °C, and was held at 300 °C for 1 min. The injection port temperature was maintained at 250 °C. Helium (99.999% purity) was used as the carrier gas at a constant flow rate of 1 mL/min.

Injection and MS parameters

A 1 µL aliquot of the sample was introduced in splitless mode. Mass spectra were acquired under electron impact ionization (EI) mode over a scan range of 0.6-1091 m/z. Data acquisition and processing were performed using MassHunter software. Compound identification was performed by matching acquired EI spectra against the NIST20 mass spectral library. Retention time (RT), molecular formula (where reported), spectral match score, and relative peak contribution (Area%-T) were recorded. Relative abundance was calculated by peak area normalization as provided in the instrument report.

Identification confidence and artifact screening

GC-MS identifications were treated as putative and interpreted using match score strength and chemical plausibility. To strengthen quality characterization, each reported compound was screened for the likelihood of being an analytical artifact or contaminant based on known GC-MS background contributors (e.g., siloxanes from column/septa bleed and plasticizer-related ester contaminants from laboratory plastics). Compounds classified as likely artifacts were not used for mechanistic mapping to CRS and were retained only for transparency as part of analytical quality reporting.

Fourier Transform Infrared Spectroscopy (FTIR)

Instrumentation and spectral acquisition

FTIR spectral analysis was performed using a Thermo Fisher Nicolet iS5 FTIR spectrometer operating in the mid-infrared range of 550-4000 cm^{-1}. Spectra were acquired at a resolution of 4 cm^{-1} with 32 cumulative scans per sample. A background spectrum was recorded prior to each measurement to support baseline correction.

Sample preparation (KBr pellet method)

For FTIR analysis, a small quantity of the sample (or dried residue where applicable) was thoroughly mixed with spectroscopic-grade potassium bromide (KBr) in a 1:100 ratio (w/w). The mixture was compressed into a translucent pellet using a hydraulic press, and the pellet was placed in the FTIR sample holder for spectral acquisition.

FTIR peak extraction and functional group assignment

FTIR peaks were identified as local minima in % transmittance and tabulated. Functional group assignments were performed using standard infrared band ranges, focusing on chemical moieties commonly present in plant-derived hydroalcoholic extracts, including hydroxyl (O-H), amine (N-H), carbonyl (C=O), alkene (C=C), and ether (C-O) groups. FTIR interpretation was used as a confirmatory fingerprint to support chemical-class inference alongside GC-MS profiling.

Literature mapping for CRS mechanistic relevance

Evidence sources and selection strategy

To interpret the chemical profile in relation to CRS pathobiology, an evidence-mapping approach was applied. CRS mechanistic domains (inflammation and cytokine signaling, oxidative stress/ROS, antimicrobial and antibiofilm relevance, epithelial barrier and mucosal function, and immunomodulation) were anchored to major CRS guideline sources (EPOS 2020/2023, ICAR-RS, and AAO-HNS documents). For each putatively identified GC-MS compound, chemical identity validation (synonyms, CAS confirmation, and basic descriptors) was cross-checked using authoritative databases (PubChem, ChemSpider, HMDB, and NIST documentation where applicable). Bioactivity evidence relevant to CRS domains was then curated from PubMed-indexed and Scopus-indexed peer-reviewed literature. Only evidence linked to the compound (or its established chemical class when compound-level evidence was limited) was considered, and interpretation was restricted to cautious mechanistic plausibility statements.

Integration of GC-MS and FTIR outputs

GC-MS outputs were tabulated as RT, compound name, CAS number, match score, and Area%-T. FTIR outputs were tabulated as peak wavenumber and functional group assignment. Integrated interpretation connected GC-MS-derived chemical classes with FTIR-confirmed functional groups to generate a coherent chemical fingerprint, and mechanistic relevance to CRS was discussed only for constituents classified as likely genuine (i.e., not flagged as likely artifacts).

RESULTS AND DISCUSSION

GC-MS chemical profile of Solanum nigrum mother tincture

GC-MS profiling of Solanum nigrum mother tincture revealed a chromatographic pattern dominated by a small number of high-area constituents (Table 1). The most abundant annotated peak corresponded to a triterpenoid-type acetate, Olean-12-en-3-ol, acetate (3β) at RT 24.1868 (Area%-T 23.98; match score 78.3). Sugar-related constituents were also prominent, particularly ethyl α-D-glucopyranoside at RT 14.9447 (Area%-T 16.51; match score 80.3) and RT 15.0321 (Area%-T 12.45; match score 69.0), along with α-L-rhamnopyranose at RT 14.8573 (Area%-T 4.11; match score 71.4). A triterpenoid hydrocarbon annotation, 24-noroleana-3,12-diene at RT 22.5263 (Area%-T 10.75; match score 64.3), further supported the presence of terpenoid/triterpenoid chemical space in the semi-volatile fraction. Several additional peaks were detected that required artifact screening (Table 1) and were therefore excluded from mechanistic interpretation.

Beyond these, the profile contained moderately represented sugar-related and small-molecule constituents including α-L-rhamnopyranose (RT 14.8573; Area%-T 4.11; match score 71.4), a "tetradecahydropicene-4a-carboxylic acid, 4Me derivative" annotation (RT 25.8874; Area%-T 4.86; match score 53.8), and lower-area entries including loliolide-like lactone (RT 16.3176; Area%-T 1.60; match score 56.2), 3-methyl-decanoic acid (RT 17.9708; Area%-T 1.05; match score 51.9), and several minor peaks with lower match scores. Collectively, the detected chemical space is consistent with a hydroalcoholic plant extract that may contain carbohydrate derivatives and terpenoid-like constituents, while also highlighting the need for strict quality interpretation rules because library matches at moderate scores can be tentative16. Figure 1 presents the chemical structures of the GC-MS-annotated constituents used for mechanistic mapping. For transparency, compounds flagged as likely artifacts were not used to support CRS relevance.

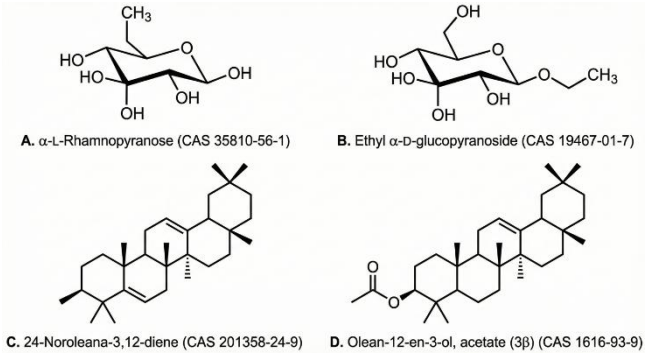

Figure 1. Chemical structures of the non-artifact constituents mapped from GC-MS profiling of Solanum nigrum homoeopathic mother tincture (Q). (A) α-L-Rhamnopyranose (CAS 35810-56-1), (B) Ethyl α-D-glucopyranoside (CAS 19467-01-7), (C) 24-Noroleana-3,12-diene (CAS 201358-24-9), and (D) Olean-12-en-3-ol, acetate (3β) (CAS 1616-93-9). Structures are shown for compounds classified as likely genuine and included in CRS mechanistic plausibility mapping; artifact-flagged peaks are reported separately in Table 1 and were excluded from this figure

Table 1. GC-MS peak profile of Solanum nigrum mother tincture (Q) with identification confidence and artifact screening

S.No	RT (min)	Putative compound (library match)	CAS No.	Area%-T	Match score	Artifact likelihood	Used for CRS mapping
1	5.1200	4-Ethylbenzoic acid, cyclopentyl ester	1000293-32-0	0.63	50.2	Possible	No (low score)
2	10.9792	Cyclohexasiloxane, dodecamethyl-	540-97-6	0.34	55.1	Likely artifact (siloxane)	No
3	12.3156	Hexanoic acid, 6-bromo-	4224-70-8	0.63	51.6	Possible	No (low score)
4	14.8573	Alpha-l-rhamnopyranose	35810-56-1	4.11	71.4	Likely genuine	Yes
5	14.9447	Ethyl α-d-glucopyranoside	19467-01-7	16.51	80.3	Likely genuine	Yes
6	15.0321	Ethyl α-d-glucopyranoside	19467-01-7	12.45	69.0	Likely genuine	Yes (cautious)
7	15.3307	(1,3-Dioxane-5,5-diyl)dimethanol, 2TMS	6228-37-1	1.61	57.7	Possible artifact (method-linked)	No
8	16.3176	Loliolide-type lactone annotation*	73410-02-3	1.60	56.2	Possible	No (low score)
9	16.7655	2,3-Bis(1-methylallyl)pyrrolidine	1000306-54-0	1.58	64.2	Possible	No (moderate score)
10	17.9708	Decanoic acid, 3-methyl-	60308-82-9	1.05	51.9	Possible	No (low score)
11	18.4078	1,4-Dibutyl benzene-1,4-dicarboxylate	1962-75-0	7.62	87.4	Possible (plastic-related)	No
12	22.5263	24-Noroleana-3,12-diene	201358-24-9	10.75	64.3	Likely genuine (class-level)	Yes (cautious)
13	23.8482	1,2-Cyclohexanedicarboxylic acid, bis(2-ethylhexyl) ester	84-71-9	12.29	62.7	Likely artifact (plasticizer-type)	No
14	24.1868	Olean-12-en-3-ol, acetate (3β)	1616-93-9	23.98	78.3	Likely genuine	Yes

15	25.8874	Tetradecahydropicene-4a-carboxylic acid, 4Me derivative	1000494-94-8	4.86	53.8	Possible	No (low score)

*Name reflects the library annotation for CAS 73410-02-3; treated as tentative due to match score.

FTIR functional group fingerprinting and alignment with the GC-MS profile

FTIR analysis provided a coherent functional group fingerprint for the tincture extract (Table 2). A broad band around 3332 cm^{-1} supports the presence of hydrogen-bonded O-H and/or N-H stretching, consistent with hydroxyl-rich chemical classes such as sugars, glycosides, phenolic-like constituents, or polyols. The peak near 2978 cm^{-1} corresponds to aliphatic C-H stretching (CH_2/CH_3), aligning with fatty acid chains and terpenoid/triterpenoid backbones.

The band at approximately 1642 cm^{-1} is compatible with C=C stretching, conjugated systems, and/or carbonyl-adjacent vibrational contributions depending on mixture context, and should be interpreted cautiously because it is not structurally specific in complex extracts. The fingerprint region peaks (1454, 1416, 1385, 1327, 1273 cm^{-1}) support bending and stretching vibrations commonly associated with aliphatic CH deformation and C-O/C-N contributions in complex matrices. Notably, the strong peaks at 1084 and 1045 cm^{-1} are characteristic of C-O stretching patterns frequently observed in carbohydrate and glycosidic systems, providing orthogonal support to the GC-MS annotation of rhamnose and ethyl glucopyranoside. The band near 876 cm^{-1} may reflect out-of-plane vibrations (often observed in substituted alkene/aryl patterns or glycosidic ring modes depending on composition) and again is best treated as supportive fingerprinting rather than definitive assignment.

Taken together, FTIR corroborates the presence of (i) hydroxyl-rich chemical space consistent with sugar/glycoside-type constituents and (ii) aliphatic chain chemistry consistent with terpenoid/triterpenoid and fatty-acid-like constituents. This convergence strengthens the internal chemical coherence of the GC-MS and FTIR dataset, while still requiring conservative interpretation at the individual-compound level.

Table 2. FTIR peaks and functional group assignments for Solanum nigrum mother tincture (Q)

Peak (cm^{-1})	Assignment (dominant vibration)	Interpretation in extract context
3332	O-H / N-H stretching (broad, H-bonded)	Hydroxyl-rich constituents(sugars/glycosides/polyols; possible phenolic-like content)12
2978	Aliphatic C-H stretching (CH_2/CH_3)	Alkyl chains; compatible with terpenoid/triterpenoid and fatty-acid-like components2
1642	C=C stretching and/or conjugated contributions (mixture band)	Non-specific; may reflect unsaturation or conjugated systems in complex matrix18
1454	CH_2 bending / deformation	Aliphatic backbone support17
1416	CH bending / aromatic or aliphatic deformation (mixture)	Supportive fingerprint region band13
1385	CH_3 symmetric bending	Aliphatic deformation; supportive13
1327	C-O stretching / C-N contributions (mixture)	Fingerprint region support for oxygenated constituents7
1273	C-O stretching (esters/ethers)	Compatible with oxygenated terpenoids/esters and glycosidic patterns15
1084	C-O stretching (strong)	Carbohydrate/glycosidic signature support15
1045	C-O stretching (very strong)	Strong support for sugar/glycoside-type chemical space15
876	Out-of-plane vibration (mixture band)	Supportive fingerprint band; interpret cautiously

Table 3. CRS-domain plausibility mapping using only "likely genuine" GC-MS constituents

Constituent (putative)	CRS domain plausibility link (qualitative, hypothesis-generating)	Evidence level
α-L-rhamnopyranose	Supports hydroxyl-rich extract chemistry; formulation/mucosal-interface relevance rather than direct CRS mechanism claim1	Not assessed (chemical marker)
Ethyl α-D-glucopyranoside	Aligns with strong FTIR C-O bands; supports carbohydrate/glycoside-like chemical space19	Not assessed (chemical marker)
24-Noroleana-3,12-diene	Terpenoid/triterpenoid chemical space plausibly relevant to inflammation/ROS discussions at class level3	Class-level plausibility

Olean-12-en-3-ol, acetate (3β)	Dominant triterpenoid-type annotation; plausibility for multi-pathway inflammatory relevance at class level (requires functional validation)20	Class-level plausibility

Mechanistic relevance mapping to CRS pathobiology

CRS is sustained by interacting inflammatory, oxidative, epithelial barrier, and microbial persistence mechanisms. Within this framework, the chemical classes observed here allow a cautious plausibility map, provided that only constituents classified as likely genuine are used.

Terpenoid and triterpenoid annotations provide a plausible starting point for discussing inflammatory relevance in CRS6. The dominance of an oleanane-type acetate and the presence of a noroleane-type hydrocarbon are directionally consistent with chemical classes frequently explored in inflammation and redox contexts in phytochemical research. Within CRS, chronic cytokine-driven signalling and mucosal remodelling contribute to persistent oedema and mucus hypersecretion; therefore, these scaffolds warrant cautious mechanistic consideration while remaining strictly hypothesis-generating in the absence of functional assays21.

The FTIR fingerprint and GC-MS sugar-related annotations indicate a strongly oxygenated matrix, dominated by hydroxyl and C-O chemical signatures. While such constituents are not interpreted as direct CRS therapeutics, they support the chemical nature of the extract and influence solubility, polarity, and mucosal interface behaviour, which are relevant to quality characterization and formulation considerations. Importantly, the strength of the carbohydrate-related FTIR region may also act as a proxy indicator for broader glycosylated chemical space that may not be fully resolved under GC-MS conditions10.

CRS relevance often hinges on microbial persistence and biofilm biology, but the present study does not directly test antimicrobial or antibiofilm activity. Accordingly, antimicrobial and antibiofilm relevance is presented only as a rationale for follow-up validation rather than as an inferred property from profiling alone14. Future studies should therefore prioritize CRS relevant pathogens and biofilm assays to evaluate whether the mapped chemical space translates into measurable biological effects.

Artifact and contamination handling as part of quality characterization

GC-MS-based quality characterization is strengthened when it explicitly distinguishes genuine sample constituents from background signals that commonly arise during analysis. In the present dataset, siloxane-class peaks and plasticizer-type ester signals were observed and interpreted as probable analytical or handling-related contributors rather than phytochemical constituents5. For example, cyclohexasiloxane, dodecamethyl is a well-recognized signature of column or septa bleed, and bis(2-ethylhexyl) cyclohexanedicarboxylate type esters are frequently reported as plasticizer contaminants introduced from laboratory plastics. These peaks were therefore retained in Table 1 for transparency but were excluded from CRS mechanistic mapping. This approach ensures that downstream interpretation remains anchored to the most defensible chemical signals and supports the manuscript's positioning as a rigorous quality-characterization study.

Summary of integrated interpretation

Overall, GC-MS and FTIR together establish a coherent chemical fingerprint for Solanum nigrum mother tincture characterized by hydroxyl-rich signatures consistent with sugar/glycoside-related chemistry and a semi-volatile fraction enriched in terpenoid/triterpenoid annotations8. After artifact screening and match-score discipline, only likely genuine constituents were carried forward for CRS mechanistic plausibility mapping. These findings provide a standardized analytical baseline that supports focused downstream validation rather than clinical inference.

CONCLUSION

GC-MS and FTIR profiling together provide a defensible quality-characterization framework for Solanum nigrum mother tincture (Q), yielding both compound-level annotations and a supporting functional-group fingerprint. The dataset indicates a chemically oxygenated matrix with prominent carbohydrate or glycoside-like signatures and a dominant triterpenoid-type feature within the semi-volatile fraction. A key methodological outcome of this work is the explicit separation of probable analytical background contaminants from constituents considered suitable for interpretation, which strengthens the credibility of the resulting chemical profile8. From a CRS standpoint, the present findings should be viewed as a structured basis for mechanistic hypothesis generation rather than evidence of clinical action. The chemical fingerprint defined here can now be used as a reference for batch comparison and for designing targeted follow-up studies that directly test CRS-relevant endpoints, particularly microbial persistence and mucosal inflammatory signalling.

ACKNOWLEDGEMENT

The author gratefully acknowledges Vinayaka Mission's Homoeopathic Medical College and Hospital and Vinayaka Missions Research Foundation (Deemed to be University), Salem, Tamil Nadu for the conducive academic atmosphere and institutional support.

REFERENCES

1. Amroudine M., Flahaut T., Gardarin C., Christophe G., Dubessay P., Ursu A.V., Chaisemartin L., Berthon J.Y., Abdelkafi S., Michaud P., Pierre G., Sustainable Sourcing of l-Rhamnose-Rich Polysaccharides from Natural Biomass Diversity: Extraction, Primary Structural Elucidation, and Antioxidant Activity, Polysaccharides, 7, 4 (2026)
2. Câmara J.S., Perestrelo R., Ferreira R., Berenguer C.V., Pereira J.A.M., Castilho P.C., Plant-Derived Terpenoids: A Plethora of Bioactive Compounds with Several Health Functions and Industrial Applications—A Comprehensive Overview, Molecules, 29, 3861 (2024)
3. Chen H.D., Yang S.P., Liao S.G., Zhang C.R., Yue J.M., Three New 24-Noroleanane Triterpenoids from Quercus aliena var. acuteserrata, Helv. Chim. Acta, 89, 1971-1977 (2006)
4. Chen X., Dai X., Liu Y., Zhang N., et al., Solanum nigrum Linn.: An Insight into Current Research on Traditional Uses, Phytochemistry, and Pharmacology, Front. Pharmacol., 13, 918071 (2022)
5. Czogała J., Pankalla E., Turczyn R., Recent Attempts in the Design of Efficient PVC Plasticizers with Reduced Migration, Materials, 14, 844 (2021)
6. Del Prado-Audelo M.L., Cortés H., Caballero-Florán I.H., González-Torres M., Escutia-Guadarrama L., Bernal-Chávez S.A., Giraldo-Gomez D.M., Magaña J.J., Leyva-Gómez G., Therapeutic Applications of Terpenes on Inflammatory Diseases, Front. Pharmacol., 12, 704197 (2021)
7. Delrue C., Speeckaert R., Oyaert M., Kerre T., Rottey S., Coopman R., Huvenne W., De Bruyne S., Speeckaert M.M., Infrared Spectroscopy: A New Frontier in Hematological Disease Diagnosis, Int. J. Mol. Sci., 24, 17007 (2023)
8. Garnepudi S.L., Pugalendhi L., Sankari A., Devi A.U.N., Raveendran M., Kalarani M.K., Deciphering Metabolite Profiling in Grafted Solanum nigrum: A Comprehensive GC-MS and FTIR Analysis, J. Appl. Hortic., 25, 291-296 (2023)
9. Gong X., Han Z., Fan H., Wu Y., He Y., Fu Y., Zhu T., Li H., The Interplay of Inflammation and Remodeling in the Pathogenesis of Chronic Rhinosinusitis: Current Understanding and Future Directions, Front. Immunol., 14, 1238673 (2023)
10. Goulet D.R., Atkins W.M., Considerations for the Design of Antibody-Based Therapeutics, J. Pharm. Sci., 109, 74-103 (2020)
11. Hossain R., Quispe C., Khan R.A., Saikat A.S.M., Ray P., Ongalbek D., Yeskaliyeva B., Jain D., Smeriglio A., Trombetta D., Kiani R., Kobarfard F., Mojgani N., Saffarian P., Ayatollahi S.A., Sarkar C., Islam M.T., Keriman D., Uçar A., Martorell M., Sureda A., Pintus G., Butnariu M., Sharifi-Rad J., Cho W.C., Propolis: An Update on Its Chemistry and Pharmacological Applications, Chin. Med., 17, 100 (2022)
12. Jovanović J., Jović M., Trifković J., Smiljanić K., Gašić U., Krstić Ristivojević M., Ristivojević P., Green Extraction of Bioactives from Curcuma longa Using Natural Deep Eutectic Solvents: Unlocking Antioxidative, Antimicrobial, Antidiabetic, and Skin Depigmentation Potentials, Plants, 14, 163 (2025)
13. Kassem A., Abbas L., Coutinho O., Opara S., Najaf H., Kasperek D., Pokhrel K., Li X., Tiquia-Arashiro S., Applications of Fourier Transform-Infrared Spectroscopy in Microbial Cell Biology and Environmental Microbiology: Advances, Challenges, and Future Perspectives, Front. Microbiol., 14, 1304081 (2023)
14. Manna T., Dey S., Karmakar M., Panda A.K., Ghosh C., Investigations on Genomic, Topological and Structural Properties of Diguanylate Cyclases Involved in Vibrio cholerae Biofilm Signalling Using in Silico Techniques: Promising Drug Targets in Combating Cholera, Curr. Res. Struct. Biol., 9, 100166 (2025)
15. Masyita A., Mustika Sari R., Dwi Astuti A., Yasir B., Rahma Rumata N., Emran T.B., Nainu F., Simal-Gandara J., Terpenes and Terpenoids as Main Bioactive Compounds of Essential Oils, Their Roles in Human Health and Potential Application as Natural Food Preservatives, Food Chem. X, 13, 100217 (2022)
16. Pandey K., Paul A., Kumar M., Tayeng D., Chattopadhyay P., Zaman M.K., Rudrapal M., Khan J., Phytochemical Profiling and Anti-Diabetic Study of Hydroalcoholic Leaf Extract of Swietenia macrophylla King, Biochem. Biophys. Rep., 43, 102200 (2025)
17. Rahimi E., Yamachi Y., Ayane Y., Kawasaki Y., Hydrated Cement Paste-Methylcellulose Composite and Its Characterization Using FTIR Spectroscopy, Proceedings of the 9th International Conference of EURO ASIA Civil Engineering Forum - Volume 1, Springer Nature, 357-366 (2026)
18. Saito K., Xu T., Ishikita H., Correlation between C=O Stretching Vibrational Frequency and pKa Shift of Carboxylic Acids, J. Phys. Chem. B, 126, 4999-5006 (2022)
19. Sansenya S., Mansalai P., Payaka A., Puttasoon C., Buddhakala N., Kongdin M., Chumanee S., Ethyl α-D-Glucopyranoside the First Report in Rice and Its Inhibitor for Acetylcholinesterase by In Vitro, In Silico and Fluorescence Analysis, Food Biosci., 68, 106641 (2025)
20. Senol H., Ozgun-Acar O., Dağ A., Eken A., Guner H., Aykut Z.G., Topcu G., Sen A., Synthesis and Comprehensive In Vivo Activity Profiling of Olean-12-en-28-ol, 3β-Pentacosanoate in Experimental Autoimmune Encephalomyelitis: A Natural Remyelinating and Anti-Inflammatory Agent, J. Nat. Prod., 86, 103-118 (2023)

21. Shen Y., Huang S., Kang J., Lin J., Lai K., Sun Y., Xiao W., Yang L., Yao W., Cai S., Huang K., Wen F., Management of Airway Mucus Hypersecretion in Chronic Airway Inflammatory Disease: Chinese Expert Consensus (English Edition), Int. J. Chron. Obstruct. Pulmon. Dis., 13, 399-407 (2018)
22. Sun N., Ogulur I., Mitamura Y., Yazici D., Pat Y., Bu X., Li M., Zhu X., Babayev H., Ardicli S., Ardicli O., D'Avino P., Kiykim A., Sokolowska M., van de Veen W., Weidmann L., Akdis D., Ozdemir B.G., Brüggen M.C., Biedermann L., Straumann A., Kreienbühl A., Guttman-Yassky E., Santos A.F., Del Giacco S., Traidl-Hoffmann C., Jackson D.J., Wang D.Y., Lauerma A., Breiteneder H., Zhang L., O'Mahony L., Pfaar O., O'Hehir R., Eiwegger T., Fokkens W.J., Cabanillas B., Ozdemir C., Kistler W., Bayik M., Nadeau K.C., Torres M.J., Akdis M., Jutel M., Agache I., Akdis C.A., The Epithelial Barrier Theory and Its Associated Diseases, Allergy, 79, 3192-3237 (2024)
23. Thakar M.S., Kearl T.J., Malarkannan S., Controlling Cytokine Release Syndrome to Harness the Full Potential of CAR-Based Cellular Therapy, Front. Oncol., 9, 1529 (2020)
24. Vlaminck S., Acke F., Scadding G.K., Lambrecht B.N., Gevaert P., Pathophysiological and Clinical Aspects of Chronic Rhinosinusitis: Current Concepts, Front. Allergy, 2, 741788 (2021)